Journal of ELECTRONIC MATERIALS, Vol. 44, No. 6, 2015
DOI: 10.1007/s11664-015-3668-x

Thermoelectric Power-Generation Characteristics of PEDOT:PSS Thin-Film Devices with Different Thicknesses on Polyimide Substrates

HIROAKI ANNO,[1,2,5] TAKAHIKO NISHINAKA,[3] MASAHIRO HOKAZONO,[1] NOBUAKI OSHIMA,[1,2] and NAOKI TOSHIMA[2,4]

1.—Department of Electrical Engineering, Tokyo University of Science, Yamaguchi, 1-1-1 Daigaku-dori, Sanyo Onoda 756-0884, Japan. 2.—Advanced Materials Institute, Tokyo University of Science, Yamaguchi, 1-1-1 Daigaku-dori, Sanyo Onoda 756-0884, Japan. 3.—Graduate School of Engineering, Tokyo University of Science, Yamaguchi, 1-1-1 Daigaku-dori, Sanyo Onoda 756-0884, Japan. 4.—Department of Applied Chemistry, Tokyo University of Science, Yamaguchi, 1-1-1 Daigaku-dori, Sanyo Onoda 756-0884, Japan. 5.—e-mail: anno@rs.tus.ac.jp

We fabricated cast films of complexes of poly(3,4-ethylenedioxythiophene) and polystyrene sulfonic acid (PEDOT:PSS) at various thicknesses, t = 3–20 μm, on flexible polyimide substrates, and studied their thermoelectric properties. We also fabricated in-plane film devices consisting of five couples of PEDOT:PSS and Ag electrodes, measuring their output power characteristics as a function of film thickness. The Seebeck coefficient and electrical conductivity of a PEDOT:PSS film with a thickness of ~20 μm on a polyimide substrate were ~15 μV/K and 500 S/cm, respectively, near room temperature. As the film thickness decreased from ~10 μm to 3 μm, the electrical conductivity increased remarkably to 1200 S/cm, while the Seebeck coefficient remained almost constant with film thickness. The maximum electric power for an in-plane PEDOT:PSS film device with a thickness of 10 μm was 1.3 μW at ΔT = 100 K. Its open-circuit voltage was 7.3 mV, and its internal resistance was 11 Ω. The measured power-generation characteristics of the film device agreed with values estimated from the dependence of thermoelectric properties on film thickness for PEDOT:PSS films on polyimide substrates. Assuming single PEDOT:PSS legs, defined as the direction of heat transport, we estimated the expected electrical power density at ΔT = 100 K as ~650 μW/cm^2 for a film thickness t = 10 μm, and 1400 μW/cm^2 for t = 3 μm.

Key words: Conducting polymer, PEDOT:PSS, thermoelectric device, power-generation characteristics, film thickness dependence

INTRODUCTON

Thermoelectric power generation, the direct conversion of heat to electric energy by the Seebeck effect, is a promising means of harvesting electricity from heat sources with low-temperature gradients relative to the environmental temperature.[1] The conversion efficiency of thermoelectrics can be described by the thermoelectric figure of merit (ZT), given by $ZT = S^2\sigma T/\kappa$, where S is the Seebeck coefficient, σ is the electrical conductivity, κ is the thermal conductivity, and T is the absolute temperature. Recently, conducting polymers have attracted much interest for use in thermoelectric applications in converting environmental energy. These polymers are attractive because they have good electrical conductivity, as high as ~1000 S/cm,[2–7] and intrinsically low thermal conductivity, usually a few orders of magnitude lower than that of inorganic materials,[8] and they consist of abundant and harmless elements. Moreover, the possibility of

(Received August 13, 2014; accepted January 24, 2015; published online February 24, 2015)

fabricating these polymers using solution processing enables printing technologies, which allow mass production of large-area materials on flexible substrates at very low cost. Doing initial research on organic thermoelectric materials, Yan et al.[9,10] reported polyaniline as a promising candidate for organic thermoelectric applications. Recently, many resarchers have studied the polythiophene system to improve thermoelectric properties,[11–24] finding it to have considerable potential. Bubnova et al.[13] reported $ZT = 0.25$ at room temperature for poly(3,4-ethylenedioxythiophene) doped with tosylate (PEDOT:TOS); in a later work, they suggested that improving the structural order of the material will improve its power factor.[20] Kim et al.[17] reported that a thin film of poly(3,4-ethylenedioxythiophene) complexed with polystyrene sulfonic acid (PEDOT:PSS) had $ZT = 0.42$ at room temperature.

Beyond these materials, it is practically important to fabricate flexible thermoelectric devices made from PEDOT:PSS and to characterize their power-generating properties, including the thermal stability and durability of the device.[25–30] Some have fabricated flexible PEDOT:PSS devices and characterized them. In particular, we have reported preparing PEDOT:PSS films on a flexible polyimide substrate, investigating their flexibility and thermal stability with respect to their thermoelectric properties.[30]

In the present study, we prepared PEDOT:PSS films with various thicknesses on a flexible polyimide substrate by a solution processing and investigated how their thermoelectric properties depended on film thickness. We also fabricated flexible in-plane film devices consisting of PEDOT:PSS legs in a practical range of film thicknesses (a few to a few tens of micrometers) and Ag electrodes, and measured their power-generation properties. The output power density of the devices increased markedly across film thicknesses of 3–10 μm, caused by an increase in electrical conductivity with decreasing film thickness.

EXPERIMENTAL PROCEDURE

PEDOT:PSS (Clevios PH1000; Heraeus Precious Metals, Leverkusen, Germany, 1:2.5 mass ratio) and 5 vol.% dimethyl sulfoxide (DMSO) were mixed by stirring for 1 h to enhance electrical conductivity.[31] The mixed solutions were cast onto a flexible polyimide substrate. To change the film thickness, the volume of solution cast was varied from 3 μL/cm^2 to 30 μL/cm^2. The films were dried slowly in air on a hot plate at ~313 K for 15 h, removing most of the water. The resultant films were further dried under vacuum at ~383 K for 2 h, removing most of the DMSO. The film thicknesses were typically 3–20 μm. The film thickness was measured by using a linear gauge (Model LGK-0110, Series No. 542-158, resolution: 0.1 μm; Mitsutoyo, Kawasaki, Japan), subtracting the thickness of polyimide substrate measured before casting from the total thickness of the cast film and polyimide substrate. Flexible devices composed of these PEDOT:PSS films at various thicknesses were prepared on a polyimide film, on which Ag electrodes were formed using a printing technique. Figure 1 shows (a) a schematic and (b) a photograph of a flexible device composed of the PEDOT:PSS films on a polyimide substrate. The device consists of five thermocouples, a leg of PEDOT:PSS with length $L = 5$ mm, width $w = 4$ mm, and thickness $t = 3$–20 μm, as well as a leg with an Ag electrode with $L = 5$ mm, $w = 3$ mm, and $t = \sim 15$ μm.

The microstructure of cross-sections of the PEDOT:PSS films on polyimide substrate was observed by field emission scanning electron microscopy (FE-SEM, S-4800, Hitachi High-Technologies Corp., Tokyo, Japan) for selected samples. The preparation method of specimens for SEM observation of cross-sections was as follows: the PEDOT:PSS films were carefully peeled off the polyimide substrate, then they were frozen in liquid nitrogen and broken into pieces in liquid nitrogen to avoid any change of microstructure of cross-sections due to shear stress by cutting.

We measured the Seebeck coefficient and electrical conductivity simultaneously at ~300–400 K by using a thin-film measurement system (ZEM 3-M8; ADVANCE RIKO, Inc., Yokohama, Japan). The experimental error in these measurements for a standard sample (constantan) was less than ±7% and ±10% for the Seebeck coefficient and electrical conductivity, respectively. The electrical conductivity was also measured with a standard four-probe method with a direct-current power supply of 0.1–0.5 mA. The Seebeck coefficient was obtained from measuring thermoelectromotive force as a function of temperature difference within a range of 5 K. We obtained the absolute Seebeck coefficient by subtracting the Seebeck coefficient of the Pt probe wire from the Seebeck coefficient, calculated from the measured thermoelectromotive force and temperature difference over the entire temperature range.

To measure the power-generation properties of a PEDOT:PSS-based flexible device, we heated one side of the device using a cartridge heater (the temperature of cartridge heater block was up to 473 K); simultaneously, we cooled the other side by circulating water at constant temperature of 293 K. A polyimide sheet was inserted between PEDOT:PSS device and cartridge heater block for insulating. Thermal conducting past was used to reduce the thermal resistance between the interfaces. We set the temperature difference ΔT to ~100 K in an in-plane direction between the two sides of the device. The temperature difference ΔT of the surface of the device was measured by a thermal imaging camera (Model T640; FILR Systems Japan, Tokyo, Japan). The surface temperature of the hot side was typically below 423 K. The output power

characteristics of the device were evaluated in air using a homemade system; this system measured the voltage–current and output power–current curves by varying a potentiometer (load resistance R_L) from 0 to 100 Ω.

RESULTS AND DISCUSSION

Figures 2, 3, and 4 show the temperature dependence of the Seebeck coefficient S, electrical conductivity σ, and power factor, respectively, over two heating and cooling cycles for the PEDOT:PSS films of different thicknesses on polyimide substrates. As shown, the data of S, σ and power factor for two heating and cooling cycles are almost the same for the PEDOT:PSS films of different thicknesses on polyimide substrates. It is expected that these PEDOT:PSS films are thermally stable up to 380 K, in agreement with our recent study of thermal stability with respect to the thermoelectric properties for PEDOT:PSS films on polyimide substrate.[30] According to the study, relatively high thermal stability and durability with respect to S and σ for PEDOT:PSS films were demonstrated by test of heating and cooling cycle (330–380 K, 30 times) and by thermal hysteresis of σ (353 K in air for 4000 h).[30] In addition, differential scanning calorimetry (DSC) from 263 K to 523 K showed no indication of a well-defined glass-transition temperature or decomposition.[30]

For all films, S was ~15.6 μV/K near room temperature, almost independent of the film thickness, and increased slightly with increasing temperature. In contrast, σ depended much on film thickness and decreased slightly with increasing temperature, causing the power factor to increase with decreasing film thickness. Figure 5 plots S and σ near room temperature as functions of film thickness for the PEDOT:PSS films on polyimide substrates. At film thicknesses greater than ~10 μm, σ was almost constant at 500–600 S/cm. As the film thickness

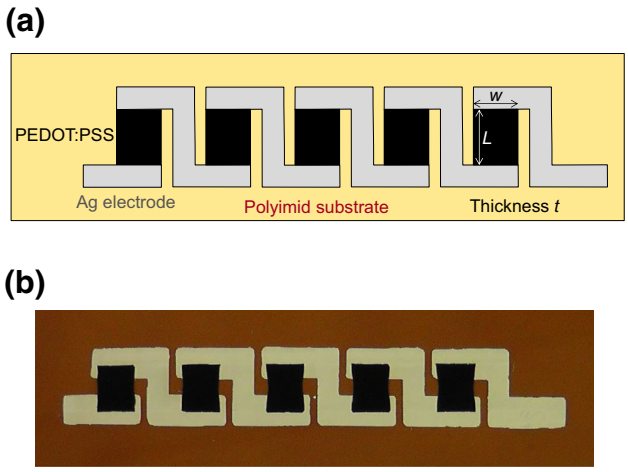

Fig. 1. (a) Schematic and (b) photograph of a PEDOT:PSS device on a polyimide substrate.

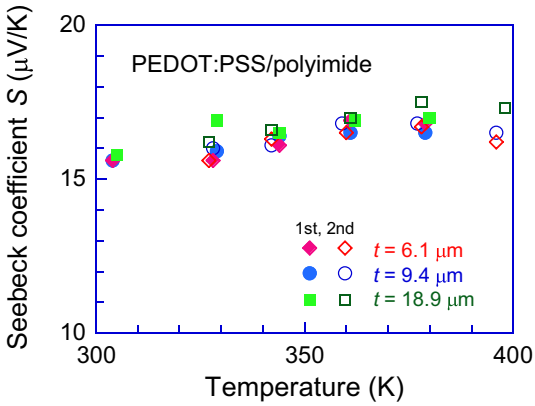

Fig. 2. Temperature dependence of the Seebeck coefficient S for PEDOT:PSS films with different thicknesses on polyimide substrates. These data are from two measurement cycles: solid and open symbols are the first and the second runs, respectively.

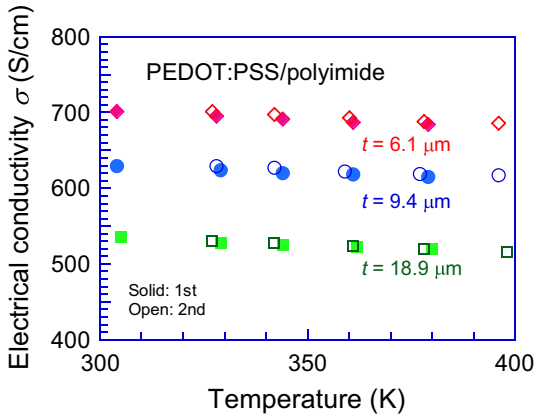

Fig. 3. Temperature dependence of electrical conductivity σ for PEDOT:PSS films with different thicknesses on polyimide substrates These data are from two measurement cycles: solid and open symbols are the first and the second runs, respectively.

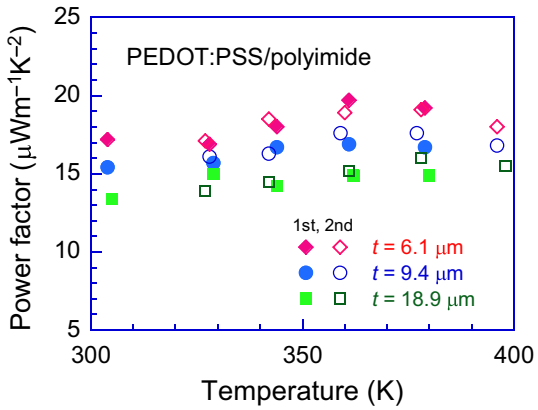

Fig. 4. Temperature dependence of the power factor for PEDOT:PSS films with different thicknesses on polyimide substrates. These data are from two measurement cycles: solid and open symbols are the first and the second runs, respectively.

decreased to less than 10 μm, σ increased markedly to 1200 S/cm at ~3 μm, but S remained almost constant. It has been reported that S and σ values near room temperature were typically 15–17 μV/K and 700–900 S/cm respectively for spin-coated PEDOT:PSS ultrathin films (thickness less than ~200 nm) with DMSO or ethylene glycol (EG) treatment and without dedoping treatment.[18,21] Our data of S for different thicknesses agree well with the reported S values and our data of σ at film thickness less than ~5 μm are comparable to the reported σ values for spin-coated ultrathin films.[18,21] In conducting polymers, thermoelectric properties may be considerably modified by oxidation level, chain alignment, interchain interaction, conjugation length, degree of structural order, and so on.[13,20] The modification of oxidation states (bipolaron, polaron, neutral) of PEDOT by chemical dedoping with counter ions or reduction agents, such as tosylate (TOS), tetrakis(dimethylamino) ethylene (TDAE), NaOH, NH_4OH, ethanolamine, ammonia solutions, hydrazine, and so on,[13,19,21–24] is crucial for the increase of Seebeck coefficient, which is, however, normally accompanied by the decrease of electrical conductivity. In contrast, the organic polar solvents, such as DMSO and EG,[16,18,21] as secondary dopants for PEDOT:PSS, significantly affect the film morphology, resulting in high electrical conductivity. It was reported by Luo et al.[18,21] that DMSO or EG treatments for spin-coated ultrathin films were able to trigger the phase separation between the conducting PEDOT chains and insulating PSS chains, leading to the formation of elongated, well-connected networks of lager PEDOT-rich grains for high electrical conductivity (up to 900 S/cm), and did not affect the chemical structure of PEDOT chains, only the morphology. According to their report, for the PEDOT:PSS films on polyimide substrate, it is suggested that the oxidation level, i.e. the carrier concentration, of the PEDOT:PSS films is almost independent of the film thickness because the Seebeck coefficient is almost unchanged, but the film morphology depends on the film thickness and plays a major role for increased electrical conductivity.

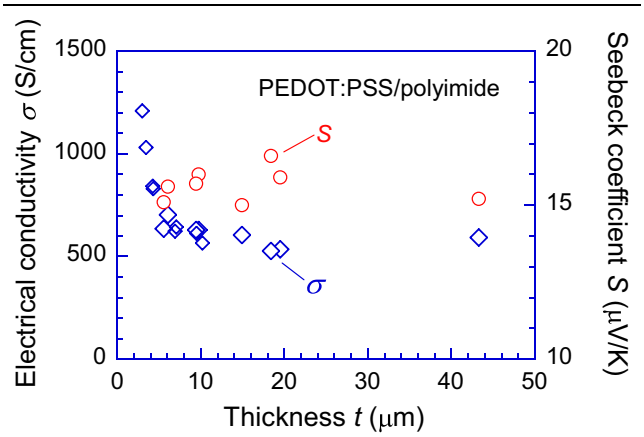

Fig. 5. Seebeck coefficient S and electrical conductivity σ near room temperature as functions of film thickness t for PEDOT:PSS films on polyimide substrates.

To investigate the correlation between the film morphology and the electrical conductivity, we observed the cross-sections of the PEDOT:PSS films with different thicknesses, as presented in Fig. 6. At the film thickness of 43 μm (σ = 593 S/cm) (Fig. 6g–j), uniform texture without any obvious anisotropic structure was observed in the upper area (film surface side), middle area, and lower area (substrate side). At the film thickness of 5.5 μm (σ = 635 S/cm) (Fig. 6d–f), the slightly ordered and elongated grains along the substrate were clearly observed. At the film thickness of 3.4 μm (σ = 1030 S/cm) (Fig. 6a–c), the marked change of morphology was observed as the ordered and elongated grains, lamella structure, along the substrate, all over the cross-section. Thus, the ordered structure of grains along the substrate may account for the increase in electrical conductivity at the film thickness less than ~5 μm.

To obtain direct information of carrier mobility and carrier concentration, we attempted to measure Hall effect by the van der Pauw technique, but measuring of the Hall voltage for the PEDOT:PSS films was very challenging, and no reliable results were obtained due to low signal-to-ratio and fluctuating off-set voltage. Recently, single crystal PEDOT nanowires were grown by liquid-bridge-meditated nanotransfer printing with vapor phase polymerization, and their electrical conductivity was up to 8797 S/cm.[32] The carrier mobility μ of single crystal PEDOT nanowires was estimated to be ~88 $cm^2/(V\,s)$ assuming the carrier concentration $n = 6.23 \times 10^{20}/cm^3$, using the relationship $\sigma = en\mu$, where e is the elementary electric charge.[32] As reported by Hokazono et al.[30] from geometrical considerations, similarly to Ref. 32, we roughly estimated the carrier concentration of PEDOT:PSS films as $8.9 \times 10^{20}/cm^3$ and the carrier mobility as ~4.2 $cm^2/(V\,s)$ for σ = 600 S/cm [~8.4 $cm^2/(V\,s)$ for σ = 1200 S/cm]. This mobility value for σ = 600 S/cm is much greater than that of pristine PEDOT:PSS prepared in the absence of organic polar solvent EG [reported as 0.15 $cm^2/(V\,s)$, $5.9 \times 10^{20}/cm^3$][14] and is comparable to that of PEDOT:PSS prepared with EG [reported as 3.6 $cm^2/(V\,s)$, $8.1 \times 10^{20}/cm^3$],[14] in which the mobility was determined by terahertz and infrared-ultraviolet spectroscopy. Further, the mobility value of spin-coated PEDOT:PSS ultrathin film with EG was determined to be 1.7 $cm^2/(V\,s)$ (σ = 830 S/cm) from the conductance g_m of its single gate field effect transistor, and the carrier concentration was estimated to be the order of $10^{21}/cm^3$.[16]

Figure 7 shows the output power characteristics of a flexible PEDOT:PSS device with a film thickness of 10 μm at a temperature difference ΔT of ~100 K. The voltage–current line is linear and the

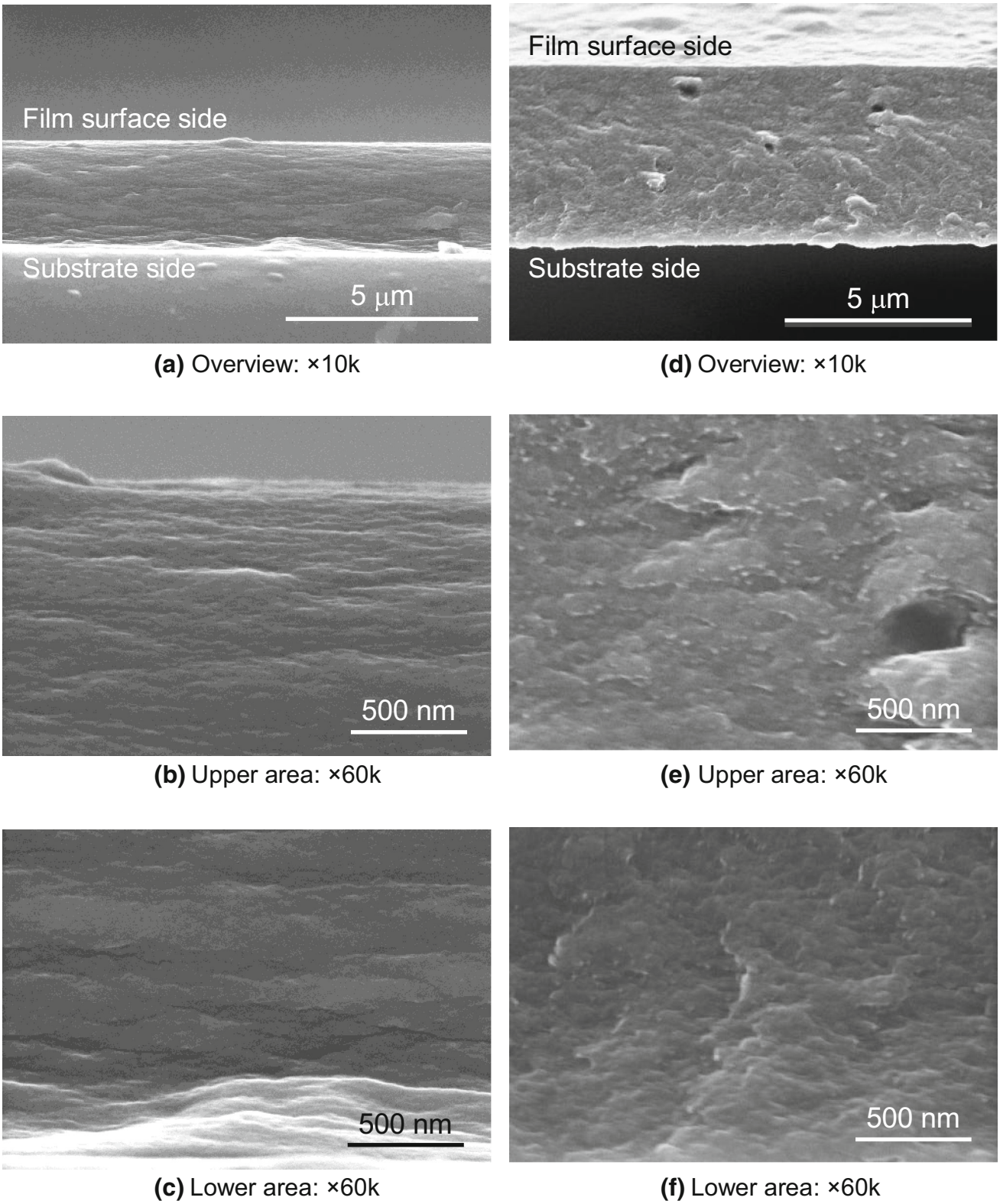

Fig. 6. SEM images of the cross-sections for PEDOT:PSS films with different thicknesses, (a)–(c) 3.4 μm, (d)–(f) 5.5 μm, and (g)–(j) 43 μm.

output power–current curve is parabolic, consistent with a general model of an equivalent power source. We obtained the internal resistance of the device R_0 from the slope of the voltage–current line, and we obtained the maximum power P_{max} from the output power–current curve at a matching condition:

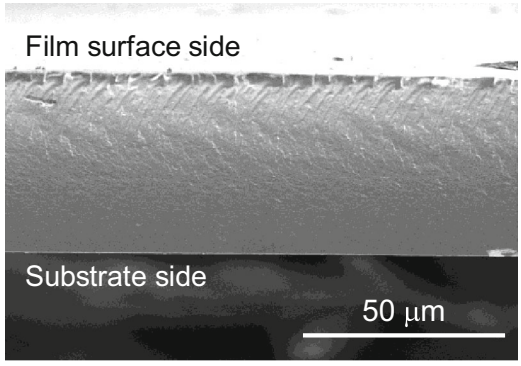

(g) Overview: ×1.0k

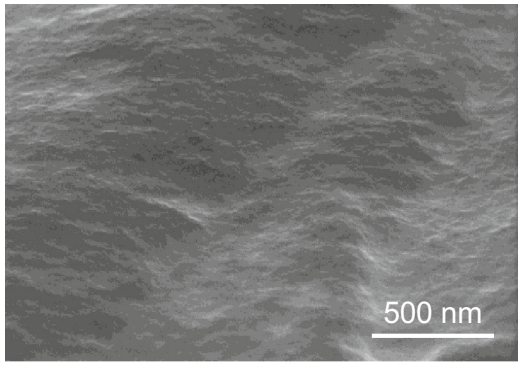

(h) Upper area: ×60k

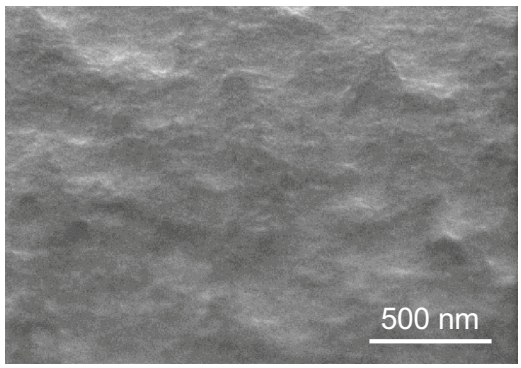

(i) Middle area: ×60k

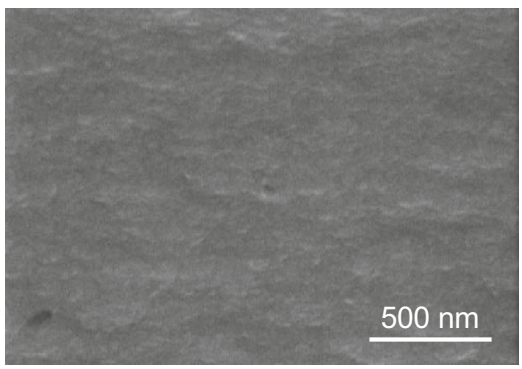

(j) Lower area: ×60k

Fig. 6. continued.

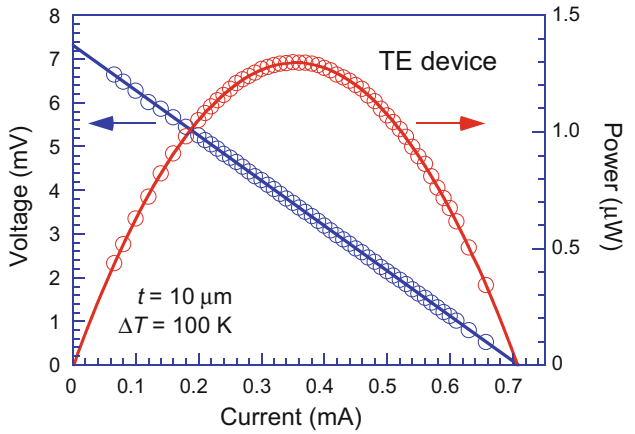

Fig. 7. Voltage–current and output power–current curves for PEDOT:PSS film at a film thickness t of 10 μm and temperature difference ΔT of ~100 K.

where the load resistance R_L equals the internal resistance of the device R_0. Table I summarizes the power-generation properties—the open-circuit voltage V_o, the internal resistance of the device R_0, the maximum power P_{max}—and the calculation of these properties from S and σ using these relationships: $V_o = NS\Delta T$, where N is the number of thermoelectric elements, $R_0 = NL/(\sigma wt)$, and $P_{max} = V_o^2/(4R_0)$ In these calculations, we used S = 15 μV/K, σ = 600 S/cm, ΔT = 100 K, N = 5, L = 5 mm, w = 4 mm, and t = 10 μm. The measured properties agree well with the calculated ones. By comparing the measured and calculated values, we deduced that the internal resistance of the device was derived mainly from the resistance of the PEDOT:PSS legs and that the interface resistance between the PEDOT:PSS and Ag electrodes was very low. Although the output power characteristics were stable during measurements, from the cycle test of the device, the drop of output power occurred due to an increase of the internal resistance of the device R_0. The increase of R_0 came mainly from the increase in the interface resistance between PEDOT:PSS and Ag electrode rather than PEDOT:PSS legs or Ag electrodes. Thus, the improvement of interface is an important technological problem to be solved for thermal stability and durability of the device.

Figure 8 shows the maximum power P_{max} as a function of film thickness for the PEDOT:PSS device at a temperature difference ΔT of ~100 K. The solid curve in Fig. 8 is P_{max} calculated by accounting for the dependence of the electrical conductivity on film thickness, as shown in Fig. 5. Figure 8 also presents calculations of P_{max} with different σ, independent of the film thickness, shown by dashed curves. P_{max} decreases monotonically with decreasing film thickness when the electrical conductivity is independent of film thickness. For example, for constant σ = 600 S/cm, P_{max} is 1.3 μW at a film thickness of 10 μm, and decreases to 0.4 μW at

Table I. Power-generation properties for a PEDOT:PSS device at a film thickness of 10 μm and a temperature difference ΔT = 100 K, as well as calculated values using measured S and σ

Property	Experiment	Calculation
Open-circuit voltage V_o (mV)	7.3	7.5
Internal resistance R_0 (Ω)	10.3	10.4
Maximum power P_{max} (μW)	1.30	1.35

Parameters of calculation: σ = 600 S/cm, S = 15 μV/K, ΔT = 100 K, N = 5, L = 5 mm, w = 4 mm, t = 10 μm.

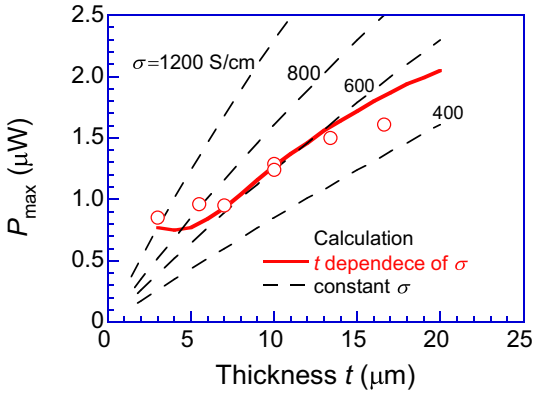

Fig. 8. Maximum output power P_{max} as a function of film thickness t for PEDOT:PSS devices at a temperature difference ΔT of ~100 K. The solid curve is a calculation that accounts for the dependence of electrical conductivity σ on film thickness, and the dashed curves are calculations at various σ, independent of film thickness.

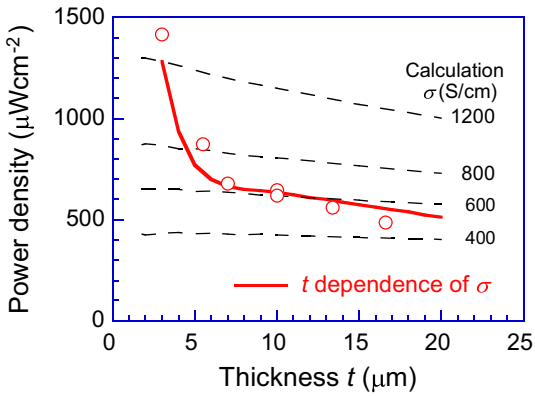

Fig. 9. Output power density as a function of film thickness t for PEDOT:PSS devices at a temperature difference ΔT of ~100 K. The solid curve is a calculation that accounts for the dependence of electrical conductivity σ on film thickness, and the dashed curves are calculations at various σ, independent of film thickness.

3 μm. In contrast, the experimental P_{max} remained high, 0.8–0.9 μW, at film thicknesses less than ~10 μm because of the marked increase in electrical conductivity of the film. This effect makes PEDOT:PSS films useful over a practical range of film thicknesses (a few to a few tens of micrometers), an advantage for use in thermoelectric devices.

Assuming an optimum packing density of single PEDOT:PSS legs, defined as the direction of heat transport, we estimated the power densities by dividing the measured P_{max} values by the cross-sectional area of PEDOT:PSS legs. These results are plotted in Fig. 9 as a function of film thickness for PEDOT:PSS devices (ΔT of ~100 K). The power density increases significantly with decreasing film thickness, at less than ~10 μm, because of the marked increase in σ with decreasing film thickness. For a film thickness of 3 μm at ΔT = 100 K, we estimated the expected electrical power density from such PEDOT:PSS devices to be ~1400 μW/cm^2.

CONCLUSIONS

We successfully prepared PEDOT:PSS films with various thicknesses on a flexible polyimide substrate by casting. Using these films, we fabricated in-plane thermoelectric devices composed of PEDOT:PSS legs and Ag electrodes. At film thicknesses greater than 10 μm, the electrical conductivity σ was ~500–600 S/cm; in contrast, at a film thickness of 3 μm, σ increased markedly to 1200 S/cm. The enhanced electrical conductivity was closely related to the modification of film morphology to ordered structure of grains along the substrate. However, the Seebeck coefficient remained nearly constant with film thickness. From the dependence of σ on film thickness, the output power P_{max} of the PEDOT:PSS device was ~1.5 μW for film thicknesses greater than 10 μm; P_{max} remained high, 0.8–0.9 μW, at t = 3 μm, because of the increased σ, even at decreased film thicknesses. The estimated power density for PEDOT:PSS device was enhanced from ~650 μW/cm^2 for t = 10 μm to 1400 μW/cm^2 for t = 3 μm at ΔT = 100 K, showing the high potential of PEDOT:PSS over a practical range of film thicknesses for use in flexible organic thermoelectric power generators.

ACKNOWLEDGEMENTS

This work was performed at the Yamaguchi Green Materials Cluster (Yamaguchi Green Valley), supported by the Regional Innovation Strategy Support Program (Global Type) of the Ministry of Education, Culture, Sports, Science and Technology (MEXT), Japan. We would like to thank UBE Industries, Ltd. for providing the polyimide films.

REFERENCES

1. D.M. Rowe, *Thermoelectrics Handbook: Macro to Nano*, ed. D.M. Rowe (CRC, Boca Raton, 2006), Section I, p.1.
2. S.J. Pomfret, P.N. Adams, N.P. Comfort, and A.P. Monkman, *Adv. Mater.* 10, 1351 (1998).
3. M. Yamaura, T. Hagiwara, and K. Iwata, *Synth. Met.* 26, 209 (1988).
4. M. Fabretto, C.J. Moncunill, J.-P. Autere, A. Michelmore, R.D. Short, and P. Murphy, *Polymer* 52, 1725 (2011).
5. C. Badre, L. Marquant, A.M. Alsayed, and L.A. Hough, *Adv. Funct. Mater.* 22, 2723 (2012).
6. Y. Xia, K. Sun, and J. Ouyang, *Adv. Mater.* 24, 2436 (2012).
7. M.V. Fabretto, D.R. Evans, M. Mueller, K. Zuber, P.H. Talemi, R.D. Short, G.G. Wallace, and P.J. Murphy, *Chem. Mater.* 24, 3998 (2012).
8. Y. Yang, *Physical Properties of Polymers Handbook*, 2nd ed. J.E. Mark (Springer, 2007), p. 155.
9. H. Yan and N. Toshima, *Chem. Lett.* 28, 1217 (1999).
10. H. Yan, N. Ohno, and N. Toshima, *Chem. Lett.* 29, 392 (2000).
11. J.-Y. Kim, J.-H. Jung, D.-E. Lee, and J. Joo, *Synth. Met.* 126, 311 (2002).
12. G. Zotti, S. Zecchin, G. Schiavon, F. Louwet, L. Groenendaal, X. Crispin, W. Osikowicz, W. Salaneck, and M. Fahlman, *Macromolecules* 36, 3337 (2003).
13. O. Bubnova, Z.U. Khan, A. Malti, S. Braun, M. Fahlman, M. Berggren, and X. Crispin, *Nat. Mater.* 10, 429 (2011).
14. M. Yamashita, C. Otani, M. Shimizu, and H. Okuzaki, *Appl. Phys. Lett.* 99, 143307 (2011).
15. C. Liu, J. Xu, B. Lu, R. Yue, and F. Kong, *J. Electron. Mater.* 41, 639 (2012).
16. Q. Wei, M. Mukaida, Y. Naitoh, and T. Ishida, *Adv. Mater.* 25, 2831 (2013).
17. G.-H. Kim, L. Shao, K. Zhang, and K.P. Pipe, *Nat. Mater.* 12, 719 (2013).
18. J. Luo, D. Billep, T. Waechtler, T. Otto, M. Toader, O. Gordan, E. Sheremet, J. Martin, M. Hietschold, D.R.T. Zahnd, and T. Gessnera, *J. Mater. Chem. A* 1, 7576 (2013).
19. F. Kong, C. Liu, H. Song, J. Xu, Y. Huang, H. Zhu, and J. Wang, *Synth. Met.* 185–186, 31 (2013).
20. O. Bubnova, Z.U. Khan, H. Wang, S. Braun, D.R. Evans, M. Fabretto, P.H. Talemi, D. Dagnelund, J.-B. Arlin, Y.H. Geerts, S. Desbief, D.W. Breiby, J.W. Andreasen, R. Lazzaroni, W.M. Chen, I. Zozoulenko, M. Fahlman, P.J. Murphy, M. Berggren, and X. Crispin, *Nat. Mater.* 13, 190 (2014).
21. J. Luo, D. Billep, T. Blaudeck, E. Sheremet, R.D. Rodriguez, D.R.T. Zahn, M. Toader, M. Hietschold, T. Otto, and T. Gessner, *J. Appl. Phys.* 115, 054908 (2014).
22. H. Park, S.H. Lee, F.S. Kim, H.H. Choi, I.W. Cheong, and J.H. Kim, *J. Mater. Chem. A* 2, 6532 (2014).
23. S.H. Lee, H. Park, S. Kim, W. Son, I.W. Cheong, and J.H. Kim, *J. Mater. Chem. A* 2, 7288 (2014).
24. M. Culebras, C.M. Gómez, and A. Cantarero, *J. Mater. Chem. A* 2, 10109 (2014).
25. R.R. Søndergaard, M. Hösel, N. Espinosa, M. Jørgensen, and F.C. Krebs, *Energy Sci. Eng.* 1, 81 (2013).
26. T. Park, C. Park, B. Kim, H. Shin, and E. Kim, *Energy Environ. Sci.* 6, 788 (2013).
27. N. Massonneta, A. Carella, O. Jaudouin, P. Rannou, G. Laval, C. Celle, and J.-P. Simonato, *J. Mater. Chem. C* 2, 1278 (2014).
28. Q. Wei, M. Mukaida, K. Kirihara, Y. Naitoh, and T. Ishida, *Appl. Phys. Express* 7, 031601 (2014).
29. M. Hokazono, H. Anno, F. Akagi, M. Hojo, and N. Toshima, *Trans. Mater. Res. Soc. Jpn* 38, 309 (2013).
30. M. Hokazono, H. Anno, and N. Toshima, *J. Electron. Mater.* 43, 2196 (2014).
31. S. Kirchmeyer, A. Elschner, K. Reuter, W. Lövenich, and U. Merker, *PEDOT: Principles and Applications of an Intrinsically Conductive Polymer* (Boca Raton: CRC, 2011), pp. 113–166.
32. B. Cho, K.S. Park, J. Baek, H.S. Oh, Y.-E.K. Lee, and M.M. Sung, *Nano Lett.* 14, 3321 (2014).